The high frequency dynamics of liquid and supercritical nitrogen

Filippo Bencivenga, Alessandro Cunsolo, Michael Krisch, Giulio Monaco, Giancarlo Ruocco, Francesco Sette

The high frequency dynamics of liquid and supercritical nitrogen

Journal:	*Philosophical Magazine & Philosophical Magazine Letters*
Manuscript ID:	TPHM-06-May-0179.R3
Journal Selection:	Philosophical Magazine
Date Submitted by the Author:	05-Sep-2006
Complete List of Authors:	Bencivenga, Filippo; ESRF Cunsolo, Alessandro; ILL Krisch, Michael; ESRF Monaco, Giulio; ESRF Ruocco, Giancarlo; Univ. of Rome, Physics Sette, Francesco; ESRF
Keywords:	liquids, X-ray scattering
Keywords (user supplied):	

The high-frequency dynamics of liquid and supercritical nitrogen

F. Bencivenga*†, A. Cunsolo‡, M. Krisch†, G. Monaco†, G. Ruocco§ and F. Sette†

† European Synchrotron Radiation Facility, B.P. 220 F-38043, Grenoble Cedex, France

‡ Istituto Nazionale di Fisica della Materia - Operative Group in Grenoble c/o Institut Laue Langevin, Grenoble, France

§ Istituto Nazionale di Fisica della Materia and Universitá La Sapienza, Roma, Italy

Inelastic X-Ray scattering has been employed to study the sound dispersion of nitrogen in its liquid and supercritical phase. In the liquid phase we clearly observe the occurrence of a positive sound dispersion associated with a structural relaxation process. Approaching the supercritical phase this phenomenon gradually disappears..

1. Introduction

The advent of third-generation synchrotron sources has allowed the development of a new high-frequency spectroscopic technique, namely inelastic X-ray scattering (IXS) [1-3]. This novel experimental tool has opened up access to previously unexplored portions of the momentum and frequency transfer (Q,ω) plane, allowing probing of the dynamics of liquids in the mesoscopic regime, i.e. at nanometer distances and picosecond timescales. A host of recent measurements have revealed that, under appropriate thermodynamic conditions, *structural* relaxation processes in liquids occur inside the IXS frequency window. These processes involve rather slow cooperative rearrangements of the local structure consequent to the perturbation induced by the propagation of density waves. When a structural relaxation is active in a fluid, the two relevant parameters ruling the fluid's dynamic behaviour are the

timescale of structural rearrangements, τ_α, and the period of the sound wave, T. If $\tau_\alpha << T$, the perturbation induced by the acoustic wave is instantaneously dissipated and the acoustic wave propagates over successive local equilibrium states of the fluid (*viscous regime*). For almost all fluids the speed of sound in this regime coincides with the adiabatic one, c_s. In the opposite limit, $\tau_\alpha >> T$, the internal degrees of freedom of the fluid are instead too slow to dissipate efficiently the energy carried by the acoustic wave, which therefore propagates elastically, i.e. without energy losses (*elastic regime*). Owing to the lack of dissipation, the speed of sound in the elastic regime, c_∞, is higher than c_s. In the intermediate (*visco-elastic*) regime the acoustic propagation is strongly coupled with the active relaxation. The sound velocity strongly depends on the frequency of the probed acoustic wave, reflected in an upwards bending of the sound dispersion relation with respect to the linear behaviour characteristic of the viscous regime (*positive sound dispersion*) [4-9].

The single-timescale assumption inherent to the visco-elastic framework is only a first approximation. The assumption that structural processes are instead characterized by a continuous distribution of relaxation timescales is, in many fluids, more reasonable. Moreover structural relaxations are not the only relaxation processes that affect the high-frequency dynamics of a liquid, but other physical processes, for example thermal diffusion, can also modify the behaviour of sound waves [10-12]. For instance, intramolecular vibrations can be responsible for the fast time decay of density fluctuations. These fast time decays are often referred to as microscopic relaxations. The phenomenology of all these processes strongly depends on the thermodynamic conditions and on the specific aggregation state of the sample.

The main aim of the present IXS study is to follow the evolution of the structural relaxation across the liquid-to-supercritical transition in nitrogen.

2. Experimental results

Nitrogen has been chosen because the two thermodynamic phases of interest (liquid and supercritical) can be easily obtained within an experimentally accessible pressure and temperature range, and because of its favourable inelastic scattering cross-section. The experiment has been performed on ID28 beamline at the European Synchrotron Radiation Facility (ESRF). The beamline was set up with an instrumental resolution function of 1.5

meV full-width-half-maximum (FWHM). The sample was embedded in a large volume, high-pressure cell kept in thermal contact with the cold finger of a cryostat. The optical windows were two 1 mm thick diamond disks, and the sample length was 10 mm. The pressure stability was better than 5 bar over the acquisition time of a typical spectrum. IXS spectra were recorded following an isobaric path (400 bar), above the nitrogen critical pressure (34 bar). The spectra were acquired at 7 different temperatures (87, 96, 107, 128, 148, 171 and 190 K) situated both above and below the critical temperature (126.2 K). Empty-cell measurements yielded a negligible contribution to the signal for all the scattering geometries used. The recorded signal is therefore proportional to the dynamic structure factor, $S(Q,\omega)$, convoluted with the instrumental resolution function. Concerning the rotational contribution to $S(Q,\omega)$, it has been simply neglected. In fact, considering a set of freely rotating diatomic molecules, the inelastic contribution associated with the transition between two rotational states J → J` have a relative intensity ~ $[j_0(Qd/2)/j_l(Qd/2)]^2$, where $d$ is the distance (0.109 nm) between the centres of mass of the two nitrogen atoms in the $N_2$ molecules and $j_l$ is the spherical Bessel functions of order l = |J-J`| [13]. For the highest value of Q explored in this experiments, the argument of the Bessel function is ~ 0.76. For this value of $Qd/2$, the relative amplitude of the leading rotational term is ~ 0.024.

The data analysis has been performed using a line-shape model derived within the framework of the memory function formalism [14,15]. In this model the dynamic structure factor is written as:

$$S(\mathrm{Q},\omega) = \frac{2c_T^2(Q)Q^2}{\omega}\,\mathrm{Im}[\omega^2 - c_T^2(Q)Q^2 - i\omega m_Q(\omega)]^{-1}, \qquad (1)$$

where $c_T(Q)$ is the Q-dependent isothermal sound velocity, and $m_Q(\omega)$ is the Fourier transform of the time-dependent memory function, which, in this context, has been approximated by:

$$m_Q(t) = [\gamma(Q)-1]c_T^2(Q)Q^2 e^{-D_T(Q)Q^2 t} + [c_\infty^2(Q) - c_s^2(Q)]Q^2 e^{-t/\tau_\alpha(Q)} + 2\Gamma_\mu(Q)\delta(t), \qquad (2)$$

where $\gamma = C_P/C_V$ is the specific-heat ratio, $D_T = \lambda/\rho C_V$ is the thermal diffusion coefficient (where λ the thermal conductivity, C_V the constant-volume specific heat and ρ the density). Γ_μ is the amplitude of the viscous dissipations induced by processes having timescales much faster than the probed experimental window and, finally, τ_α and c_∞ are the relaxation time and the high-frequency limit of the sound velocity, respectively. Following the prescriptions of molecular hydrodynamics, all the thermodynamic quantities entering eq.2 are assumed to be Q-dependent extensions of their respective macroscopic counterparts. The $\delta(t)$-function in eq.2 accounts for the fast dynamics, which induces an instantaneous time decay of $m_Q(t)$. These dynamics can be associated with relaxations, whose characteristic timescale is much shorter than the period of the probed waves. As a consequence the corresponding term in the memory function can be approximated by a $\delta(t)$-function [7,8]. The second exponential term in eq.2 accounts for the visco-elastic transition responsible for the positive sound dispersion. Finally, the first term in eq.2 accounts for the contribution of thermal diffusion to the time decay of memory function. The presence of this term allows the retrieval of the "classical" hydrodynamics result represented by the Rayleigh-Brillouin triplet at low (Q,ω) [14]. In order to account properly for the detailed balance, the symmetric lineshape obtained by inserting eq.2 in eq.1, has been multiplied by a frequency-dependent factor: $x(n(x)\text{-}1)$, where $n(x)$ is the Bose factor, $x = \hbar\omega/k_BT$ and k_B is the Boltzmann constant. Finally, the theoretical function has been convoluted with the measured instrumental resolution function, $R(\omega)$.

In the fitting routine, the parameters $\tau_\alpha(Q)$, $c_\infty(Q)$, $c_T(Q)$, $\Gamma_\mu(Q)$ and an overall intensity factor were left free. The Q-dependencies of the parameters γ and D_T have been neglected and their values have been fixed to the corresponding thermodynamic values derived from the nitrogen equation of state [16]. This assumption has been mainly motivated by the necessity to reduce the number of free parameters in the fitting routine; otherwise the correlation among them is too high in order to produce a reliable fit. The choice of these two parameters as fixed ones is based on the following considerations: i) unlike τ_α, c_∞ and Γ_μ, accurate thermodynamic values for γ and D_T are available in literature. On the other hand they cannot be generalized at finite-Q using simple relations, like for instance eq.3 for c_T. Furthermore, as pointed out by other authors [17], the Q-dependencies of these parameters may change with temperature in a non trivial way. ii) γ and D_T are mostly related to the first term on the right-hand side of eq.2, the influence of which on the memory function is, in this case, smaller than that associated with the second term of the right-hand side of eq.2. In fact

the relative amplitude of these two terms is: $[\gamma - 1]c_T^2/[c_\infty^2 - c_s^2] \sim 0.4$ with $\gamma \sim 2$ and $c_\infty \sim 1.5\ c_s$. Furthermore this ratio decreases with increasing Q, since $c_T \propto S(Q)^{-1}$ while $[c_\infty^2 - c_s^2]$ increases with Q, since the Q-softening of c_∞ is much smoother than that of c_s (see fig.2). Consequently, even if the characteristic timescale for thermal diffusion lies inside the experimental window, this process becomes dominant only when the timescale of the visco-elastic process moves out the experimental window. iii) As recently pointed out in another paper [18], when the thermal diffusion becomes the dominant process, its effect on the dispersion relations, which consists in an adiabatic to isothermal transition of sound propagation, is qualitatively well described by considering γ and D_T as Q-independent.

The parameters $c_T(Q)$ and $c_s(Q) = \gamma^{1/2} c_T(Q)$ have been also independently calculated using the finite-Q generalization of the compressibility theorem [14,15]:

$$c_T(Q) = \sqrt{k_B T / MS(Q)} \qquad (3)$$

where M is the molecular mass of nitrogen and $S(Q)$ is the static structure factor. The agreement between the two procedures can be appreciated by looking at the full lines and the black squares in fig.2. This perfect match can be considered as a check of the consistency of the fitting procedure. The static structure factor was experimentally determined by recording the energy-integrated scattering, corrected for the known nitrogen form factor, f(Q) [19], as well as for any possible geometrical effects. The absolute scale of $S(Q)$ has been provided by scaling the measured energy-integrated scattering intensity by a Q-independent factor, in order to obtain the correct $Q = 0$ (compressibility) limit of $S(Q)$ [14,15]. Such a limiting value can be directly calculated from the equation of state. Finally, the apparent sound velocity of acoustic excitations, $c_L(Q)$, has been determined using $c_L(Q) = \Omega_L(Q)/Q$, where $\Omega_L(Q)$ is the frequency of the maximum of the longitudinal current spectra: $\omega^2 S(Q,\omega)/Q^2$.

In fig.1 selected IXS spectra are compared with the corresponding best-fit line-shapes and instrumental resolution function. Each spectrum typically covers an energy transfer range of ±40 meV and has been collected at Q values between 3.5 and 14 nm^{-1}. The logarithmic plot emphasizes the overall agreement between experimental and model line shapes, even in the spectral tails.

In fig.2 we compare the apparent dispersion, $\Omega_L(Q)$ (open circles), with the infinite-frequency, $c_\infty(Q)Q$ (full circles), and the adiabatic one, $c_s(Q)Q$, for four different temperatures (87, 128, 148 and 171 K). The adiabatic dispersion has been either obtained from the fit (full squares) or calculated using eq.3 (full lines). In the same panels we also report the inverse of the structural relaxation time $1/\tau_\alpha(Q)$ (dashed lines) as derived from best-fit results. Experimental data in fig.2a clearly show that the apparent dispersion is systematically higher than the adiabatic one. Although the c_∞ limit is not fully reached, we clearly notice the presence of a positive sound dispersion, fingerprinting the occurrence of a structural relaxation process. This transition occurs in correspondence to the condition $1/\tau_\alpha(Q) \sim \Omega_L(Q)$, which represents the situation where the characteristic relaxation timescale is equal to the period of the probed sound wave. This positive sound dispersion is noticeably reduced at 128 K (panel b), where the apparent dispersion is rather close to the adiabatic one. This is most likely due to both the relatively higher values of $1/\tau_\alpha(Q)$ and the lower values of $\Omega_L(Q)$, which prevents the viscoelastic crossover being reached. After a further increase of the temperature (panels c and d), $1/\tau_\alpha(Q)$ moves out of the probed frequency window and any evidence of positive dispersion disappears. In fact, at these temperatures the apparent and the adiabatic dispersions merge into each other. A deviation of the longitudinal dispersion from the adiabatic value can be observed looking at the higher Q-values of fig.2d. This behaviour has been recently interpreted as an adiabatic-to-isothermal transition of sound propagation [18].

The other information we can derive from the data analysis is the value of the structural relaxation time. As already observed in other experiments performed in this Q-range [6-9,20-22], we found that the value of $\tau_\alpha(Q)$ decreases with increasing Q at a given temperature. As an example we report the Q-dependence of such a parameter for two selected temperatures in the inset of fig.3. The full lines through the experimental data are an interpolation performed using the empirical function: $\tau_\alpha(Q) = \tau_\alpha e^{-AQ}$. These interpolations permit one to obtain τ_α, the $Q = 0$ extrapolated value of the relaxation time. In fig.3 this quantity is plotted versus the inverse temperature. From this Arrhenius plot we can observe that τ_α first linearly decreases with temperature, and then remains almost flat for temperatures higher than the critical one (indicated by the vertical arrow). From the first decrease of τ_α we can estimate the activation energy, $E_a = 0.55 \pm 0.16$ kJ mole^{-1}, associated with the relaxation

process. This estimation is represented by the dashed line in fig.3. This very low activation energy reflects the very weak intermolecular bonds between N_2 molecules.

3. Conclusions

In conclusion our observations can be summarized as follows: i) The apparent sound branch of nitrogen shows clear signatures of a positive sound dispersion in the liquid phase, thus witnessing the presence of a structural relaxation process. ii) The timescale, τ_α, of this structural relaxation process becomes increasingly shorter as the system approaches the supercritical phase. iii) Owing to both the decrease of $\tau_\alpha(Q)$ and $\Omega_L(Q)$, the positive sound dispersion gradually disappears while reaching supercritical conditions, because the crossover condition, $1/\tau_\alpha(Q) \sim \Omega_L(Q)$, can be no longer accomplished. iv) τ_α seems to lose its typical Arrhenius temperature dependence above the critical temperature.

These findings indicate that, in the liquid phase, the high-frequency dispersive behaviour of a simple, non-associated fluid, such as nitrogen, is mainly controlled by the structural relaxation, as manifested by the presence of the positive sound dispersion. In contrast, in the supercritical phase, the role of the structural relaxation on the sound dispersion relation becomes almost negligible.

Acknowledgments

We are grateful to D. Gambetti and R. Verbeni for help in the preparation of the experiment.

References

[1] E. Burkel, *Inelastic Scattering of X-Rays with Very High Energy Resolution* (Springer-Verlag, Berlin, 1991).

[2] F.Sette *et al.*, Phys. Scr. **T66** 48-56 (1996).

[3] E. Burkel, Rep. Prog. Phys. **63** 171 (2000).

[4] G. Ruocco and F.Sette, J. Phys.: Condens. Matter **11** R259 (1999).
[5] T. Scopigno *et al.*, Rev. Mod. Phys. **77** 881 (2005).
[6] A. Cunsolo *et al.*, J. Chem. Phys. **114** 2259 (2001).
[7] G. Monaco *et al.*, Phys. Rev. E **60** 5505 (1999).
[8] E. Pontecorvo *et al.*, Phys. Rev. E **71** 011501 (2005).
[9] R. Angelini *et al.*, Phys. Rev. B, **70** 224302 (2004).
[10] J. Markham, R.T. Beyer, and R.B. Linsday, Rev. Mod. Phys. **23** 353 (1951).
[11] D. Sette, in *Encyclopedia of Physics*, edited by S. Flügge, Vol. "Acoustics I and II" (Springer-Verlag, Berlin, 1968).
[12] E. Herzfeld and T.A. Litovitz, *Absorption and Dispersion of Ultrasonic Waves* (Accademic Press, New York, 1959).
[13] A. Cunsolo *et al.*, J. Low Temp. Phys. **29** 117 (2002).
[14] J.P. Boon and S. Yip, *Molecular Hydrodynamics* (McGraw-Hill International Book Company, New York, 1980).
[15] U. Balucani and M. Zoppi, *Dynamics of the liquid state* (Clarendon Press, Oxford, 1994).
[16] Nist Database, http://webbook.nist.gov/chemistry/form-ser.html.
[17] T.Bryk and I.Mryglod, Phys. Rev. E **63** 051202 (2000).
[18] F. Bencivenga *et al.*, Europhys. Lett. **75** 70 (2006).
[19] R.V. Gopala Rao and R.N. Joarder, J. Phys. C: Solid State Phys., **12** 4129 (1979); *International Tables of X-Ray Crystallography* (Kynoch, Birmingham, 1974).
[20] T. Scopigno, U. Balucani, G. Ruocco and F. Sette, Phys. Rev. Lett. **85** 4076 (2000).
[21] T. Scopigno, U. Balucani, G. Ruocco and F. Sette, Phys. Rev. E **63** 011210 (2000).
[22] T. Scopigno *et al.*, Phys. Rev. Lett. **89** 255506 (2002).

Figure captions

Figure 1: Selection of IXS spectra of nitrogen at the indicated values of temperature and Q. The experimental data (full circles) are reported together with their best-fit lineshape (grey lines) and instrumental resolution function (black lines).

Figure 2: Dispersion curves of the longitudinal acoustic mode of nitrogen at 87, 128, 148 and 171 K. The full lines and the full squares represent the adiabatic dispersions derived, respectively, from $S(Q)$ measurements and from the fitting parameter $c_T(Q)$. The open circles

indicate the maxima of longitudinal current spectra. The dashed lines represent $1/\tau_\alpha(Q)$, which has been evaluated by interpolating the results of the performed lineshape analysis. Full circles represent the infinite-frequency sound dispersion.

Figure 3: Arrhenius plot of the $Q = 0$ extrapolated values of the structural relaxation time. In the inset, two examples of the procedure for extrapolating $\tau_\alpha(Q)$ at $Q = 0$ are illustrated.

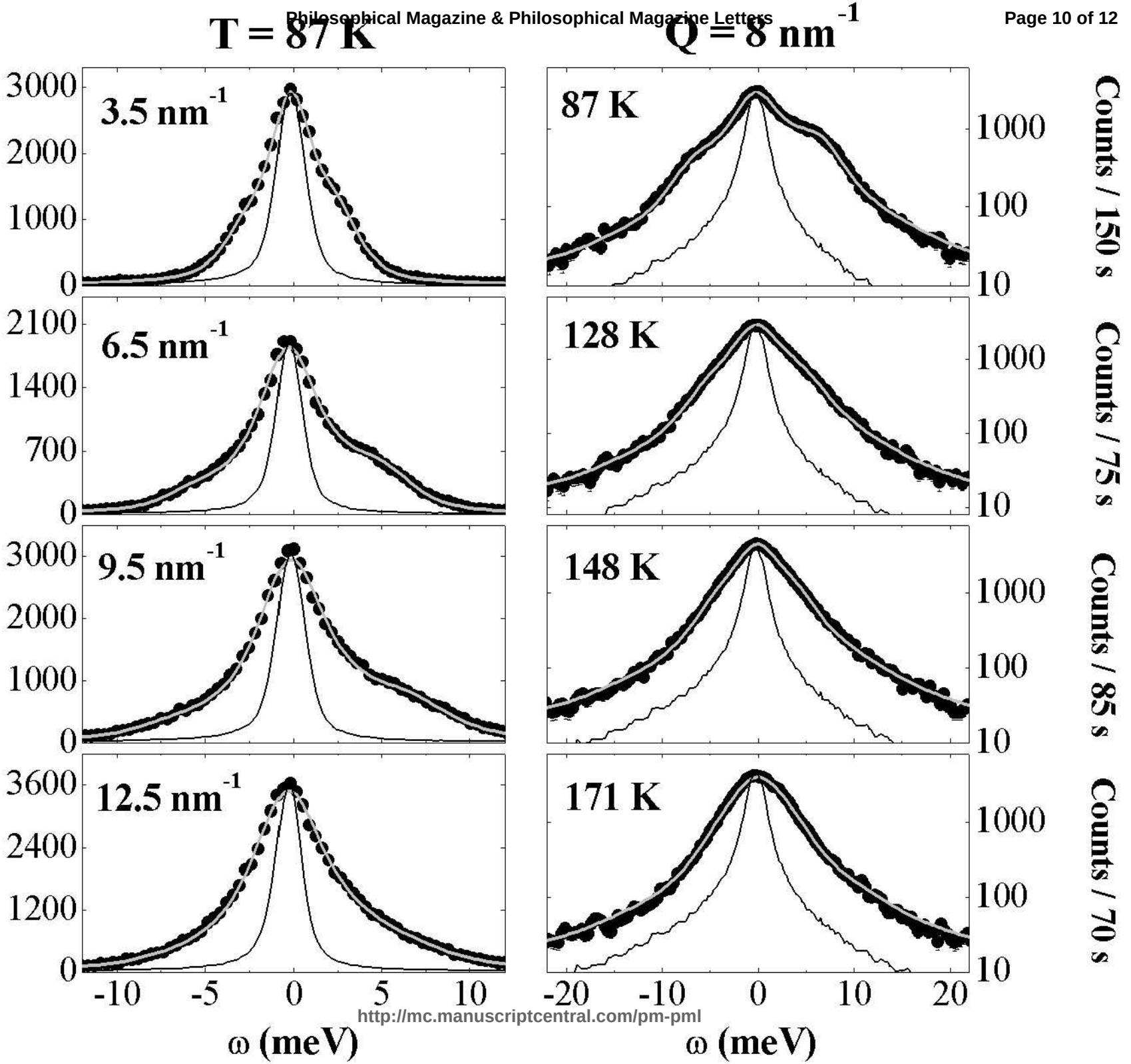
T = 87 K
Q = 8 nm^{-1}
3.5 nm^{-1}
6.5 nm^{-1}
9.5 nm^{-1}
12.5 nm^{-1}
87 K
128 K
148 K
171 K
Counts / 150 s
Counts / 75 s
Counts / 85 s
Counts / 70 s
ω (meV)
ω (meV)

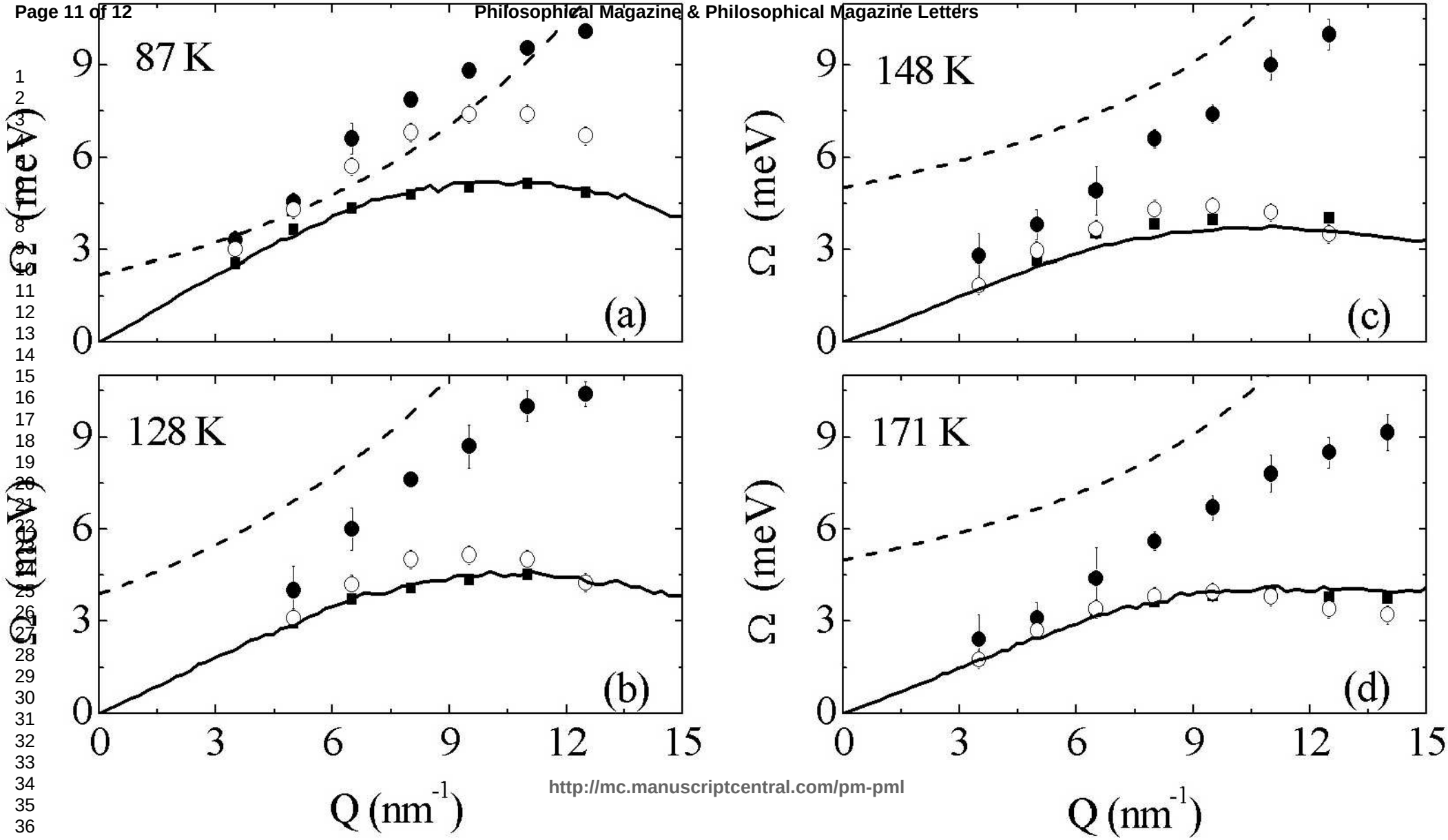
87 K
148 K
128 K
171 K
(a)
(b)
(c)
(d)
Ω (meV)
Q (nm^{-1})
0
3
6
9
12
15